

We greatly appreciate reviewer’s insightful and helpful comments regarding our manuscript. The manuscript has been revised based on reviewer’s comments. Following the reviewers’ suggestions, the revised manuscript includes a more detailed description and validation of the POP2–waves model against NOAA CT2022, as well as a clearer rationale for focusing on 12 key regions out of the 30 ocean basins. We have also expanded the discussion on marine carbon chemistry, addressed the challenges of wave-ocean coupling in the conclusions, and restructured the manuscript for improved readability. Below are the point-by-point replies to reviewer’s comments and concerns.

Sincerely,

Yung-Yao Lan, Huang-Hsiung Hsu, Wei-Liang Lee and Simon Chou

Anonymous Referee #1

The reviewer comments are formatted in italics and the authors response to the comments are formatted in bold.

Notation *RC1.P#* represents Reviewers Comment. Paragraph Number

Specific comments:

RC1.1 Consider using the revised version of K_w from Wanninkhof (2014) instead of Wanninkhof (1992).

Response:

Thank you for pointing out the mistake. In the B-CTL control experiment, the coefficient (k) for gas transfer velocity in Equation (2) follows Wanninkhof (1992), where $k = 0.31$. I mistakenly entered 0.251, which may have led to confusion with Wanninkhof (2014); this has now been corrected in the revised manuscript. For further details, please refer to the original CESM1 POP2 code (ecosys_mod.F90), specifically the annotation of the variable *xkw_coeff* (! a = 0.31 cm/hr s^2/m^2 in (s/cm)) and Table RC1.1.

Table RC1.1 The coefficient (k) used to parameterize gas transfer velocity (K_w) differs between Wanninkhof (1992) and Wanninkhof (2014).

	Wanninkhof (1992)	Wanninkhof (2014)
the coefficient (k) of gas transfer velocity (K_w) $K_w = k \langle U_{10}^2 \rangle (Sc/660)^{-0.5}$	0.31	0.251
optimal method	applicable to deduce K_w at steady winds	The optimal coefficient was obtained using an inverse modeling approach with CCMP ¹ winds and the Modular Ocean Model General Circulation Model (MOM3 GCM).

Note:¹CCMP: The Cross-Calibrated Multi-Platform (CCMP) are produced by Remote Sensing Systems (RSS) with support from a NASA Ocean Vector Winds Science Team grant.

RC1.2 L78-L87: the text on direct flux observations requires revisions. When referring to ‘direct observations’ in this context, it is usually understood ‘direct flux measurements’. However, here the authors first refer to pCO₂ observations and then to direct fluxes using eddy covariance. Please revise the text to increase clarity. Also note that direct fluxes using eddy covariance can be made with both open- and close-path analyzer, which is not mentioned in the text. Furthermore, data assimilation is mentioned here, where it seems rather isolated. Please provide the necessary information to present a sound context for the reader.

Response:

Thank you for your suggestion. The L78-L87 lacked a complete and coherent description. The revised version is as follows:

Direct flux measurements in marine environments using the eddy covariance method can be conducted with both open- and closed-path analyzers. A closed-path infrared gas analyzer (e.g., LI-7000, LI-COR) operates with an enclosed measurement chamber (Sutton et al., 2014, 2021; Bakker et al., 2016; Sabine et al., 2020; Akhand et al., 2021; Wu and Qi, 2023), whereas open-path analyzers (e.g., LI-7500, LI-COR) measure infrared absorption directly in ambient air (Edson et al., 2011; Tokoro et al., 2014; Bell et al., 2017; Dong et al., 2021; Van Dam et al., 2021). Both types are affected by H₂O cross-sensitivity, but each has its own advantages and limitations (Honkanen et al., 2018).

RC1.3. Section 2.1 should not be called ‘observational data’, this is misleading as the NOAA CarbonTracker is not only based on observations, but largely on model predictions and numerical techniques to estimate the fluxes.

Response:

We have changed the title of Section 2.1 from “Observational Data” to “Model Validation Data” and revised several sentences in this section to provide a better introduction to CarbonTracker and to avoid using the phrase “sources and sinks of CO₂ flux.”

RC1.4. As mentioned above, the methodology section requires substantial improvements. This is particularly important given that the manuscript is submitted to a model development journal. Therefore, strong emphasis should be made in presenting the relevant aspects of such model development. In this case, details about the wave module and its implementation in POP2 is of particular relevance. However, other aspects are also lacking. For example, details about the CarbonTracker, details of each of the models and model components, information about input data, forcing, etc. The authors mention pCO₂, pH and the ‘POP2 (bio)geochemistry response’ in the methodology section, but there is no information about the biogeochemical module, and this is not included in the architecture diagram in figure 1 either. This is all essential for the reproducibility of the results.

Response:

Thank you for your suggestion. We have substantially revised the methodology section of the manuscript, including (1) the development of the CESM1–POP2–waves model and its component modules (Sections 2.2 and 2.3), (2) a more detailed description of CarbonTracker (Section 2.1), (3) additional information on POP2–waves input data and atmospheric forcing (Sections 2.2 and 2.3), and (4) an expanded description of the Marine Biogeochemistry (MARBL) module in Section 2.2 and Fig. 1, highlighting that all components influence the air–sea CO₂ flux. Please refer to the revised manuscript for details of these changes.

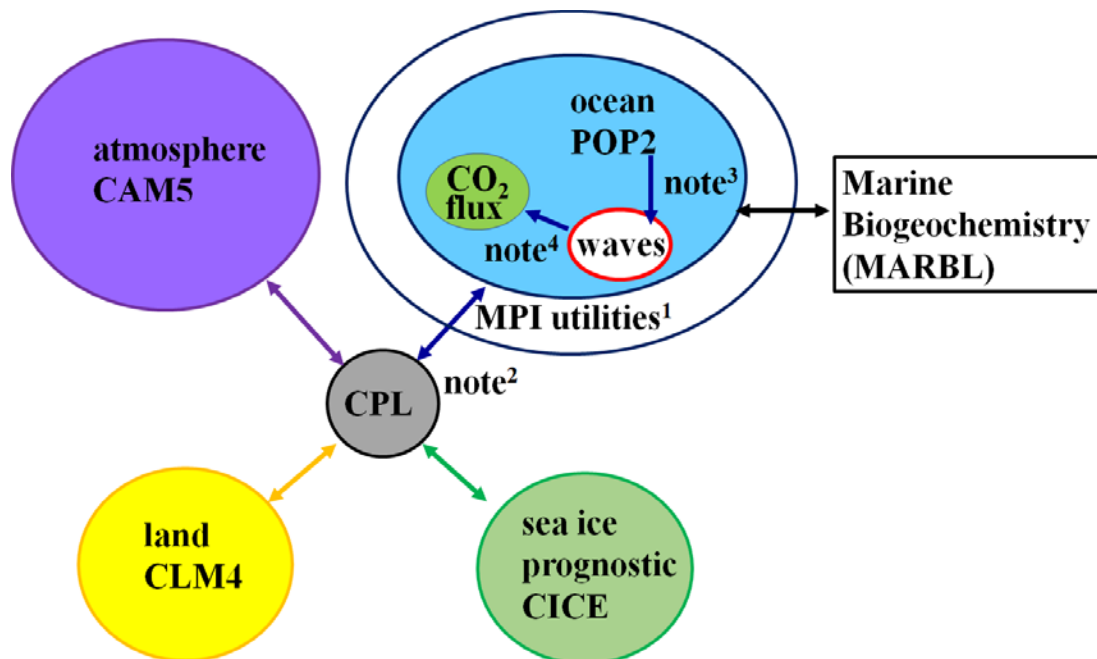


Figure 1. Architecture diagram for POP2–waves experiment in CESM1.2.2 framework, all components adhere to the CESM 1.2.2 framework, except for

certain parts of the ocean component. The model components including components for the atmosphere [Community Atmosphere Model version 5 (CAM5)], land [Community Land Model version 4 (CLM4)], ocean [Parallel Ocean Program, version 2 (POP2)], along with its associated modules—the waves module (waves) and the Marine Biogeochemistry (MARBL) module—sea ice [prognostic Los Alamos Sea Ice Model (CICE)], and the coupler (CPL).

Note:

¹The wave-module variables are communicated between neighboring blocks via MPI, including zonal and meridional 10-m winds, wave radiation stress, subsurface momentum, and wave radiation and energy densities.

²To transfer variables such as zonal and meridional 10-m winds and friction velocity (including sea surface and ice fraction) from the CPL to POP2.

³ The wave module receives variables from POP2, including the interpolation of depth-varying currents from z-coordinates (60 levels) to the wave module's vertical sigma coordinates (21 levels), along with ocean grid information in the x, y, and z directions.

⁴ The wave module outputs significant wave height and friction velocity from the CPL for calculating the bubble-mediated gas transfer velocity in Eq. (3).

RC1.5. Following on my previous comment, Section 2.3 should include much more than 10 lines on the coupling of POP2-waves. The information here should be enough for a reader to be able to reproduce the results!

Response:

In Section 2.3, we have provided more than 20 lines describing the coupling of POP2-waves. The revised manuscript explains how the wave module is integrated into POP2, including vertical coordinate transformation, required external input files, and its parallel computing implementation within the CESM1.2.2 framework, as well as the improvements shown in Fig. 1.

RC1.6. There is a notation issue that can cause confusion. The authors refer to the gas transfer velocity as K_w , often mentioning K_w from W92, i.e. eq (2). However, in eq. (3) K_w is not only the wind-based component of the parametrization, but the total gas transfer velocity (i.e. including waves), and $K_{w,NB}$ refers to wind-based component from W92, not K_w anymore. Please, use a consistent notation.

Response:

In Eqs. (2–3), K_w in both equations represents the total gas transfer velocity; in Eq. (2), it follows W92, whereas in Eq. (3), it is based on Deike and Melville (2018). In Eq. (3), K_w consists of two components: the non-bubble term ($K_{w,NB}$) and the bubble term ($k_{w,B}$). The $K_{w,NB}$ is based on the friction velocity, u_* (m s^{-1}) as shown in the shaded area of Fig. 7(d), and therefore differs from W92, which is based on the squared 10-m wind speed as shown in the shaded area of Fig. 7(c) or the Fig. RC1.6.1.

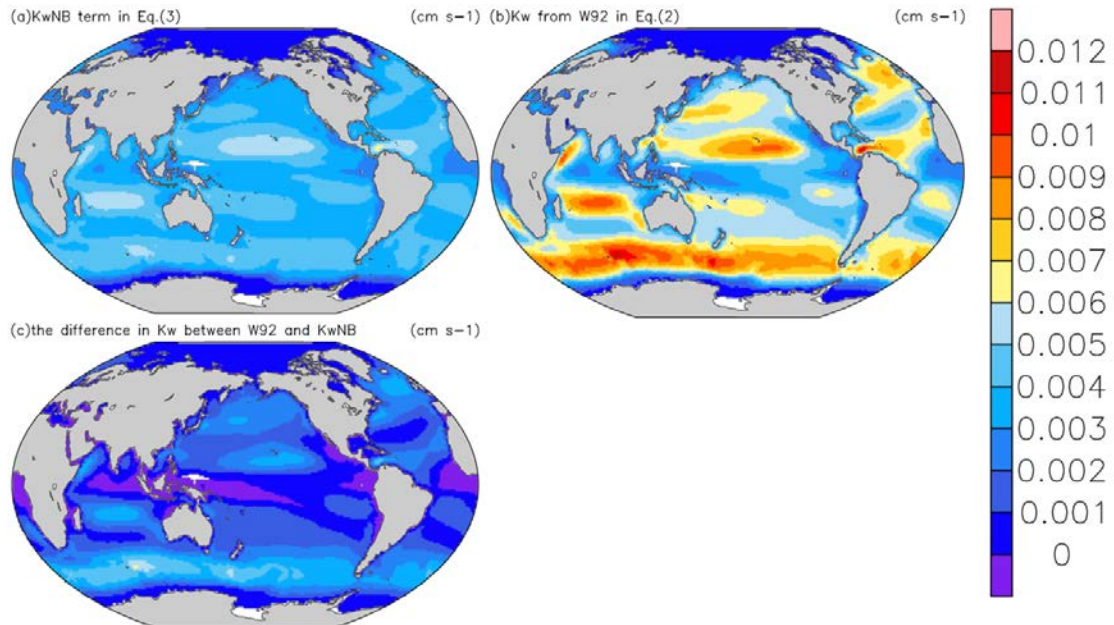


Figure RC1.6.1. The gas transfer velocity from the Eqs. (2–3), (a) the gas transfer velocity of the non-bubble-mediated term ($K_{w,NB}$), (b) K_w from W92 in Eq. (2), and (c) the difference in K_w between W92 and $K_{w,NB}$.

RC1.7. In section 3.1, a figure of the differences would be useful, e.g. B-CTL minus NOAA CT2022 and POP2-waves minus NOAA CT2022.

Response:

Yes, the differences between the model simulation and NOAA CT2022 are now clearly shown, while the original spatial distribution provides the overall positive and negative ranges of CO_2 flux in the model simulation. Please see the revised manuscript and Fig. 2(e–f) for these changes.

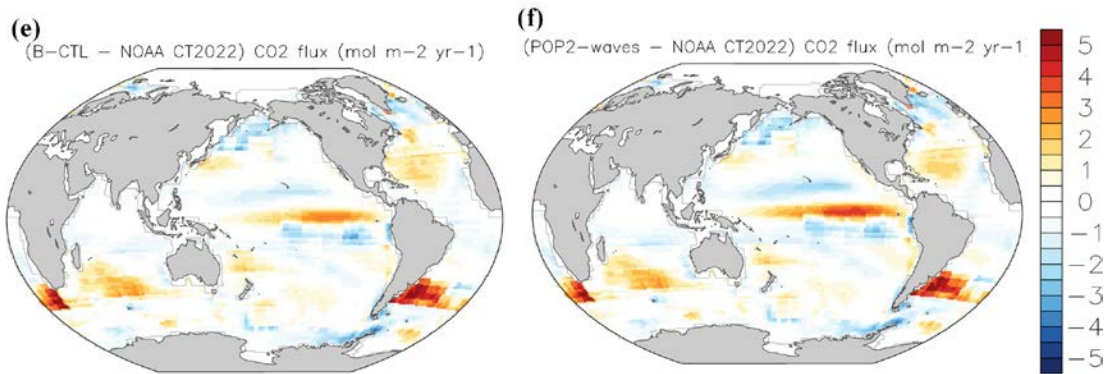


Fig. 2(e-f). Part of Fig. 2 shows the CO₂ flux differences between the model simulation and NOAA CT2022: (e) the difference between B-CTL and NOAA CT2022, and (f) the difference between POP2-waves and NOAA CT2022.

RC1.8. In figures 3, 4 and 5, having the SD in percentage represented by bars makes it very hard to get the idea of the magnitude. It would be better to find the way of having the SD along the flux or K magnitude lines.

Response:

Thank you for your comment. Figure 3 contains 9 subfigures. Plotting \pm standard deviation (SD) along the flux or K-magnitude lines for the 3 variables over 12 months would likely produce overlapping curves that are difficult to distinguish. In the revised manuscript, we present the monthly SD values directly, rather than expressing them as a percentage of the overall ranking range in Figs. 3–5, thereby avoiding overlap between the mean lines and SD markers.

RC1.9. Through the results, suddenly the NOAA CT2022 is not used anymore, why? This should be considered as the reference throughout the manuscript, as it is used in Section 3.1.

Response:

We have followed NOAA’s Global Monitoring Laboratory usage policy by appropriately acknowledging and citing NOAA CT2022 (Jacobson et al., 2023) as a reference, and we have included acknowledgments throughout the manuscript for providing the CT2022 data.

The inversion CO₂ flux in CarbonTracker CT2022 relies on meteorological fields from that are driven by the daily weather forecasts from the specialized meteorological centers of the world, specifically wind, temperature, pressure, and boundary layer dynamics. In addition, the interannual variability in the

first-guess ocean flux arises entirely from wind-speed effects on gas transfer velocity, because the ocean inversions only retrieve a long-term mean and a smooth trend (Jacobson et al., 2023).

Using alternative reanalysis data (e.g., ERA5, NCEP, or NOAA satellite products) in place of these primary fields may introduce temporal mismatches with CO₂ fluxes, which is inconsistent with the NOAA CT2022 data policy that prescribes the use of only a long-term mean and smooth trend. Consequently, sections 3.2, 3.3, and 3.4 do not attempt to compare the CO₂-meteorology interactions observed in CT2022 with those derived from other reanalysis products.

RC1.10. Please add information about how the different ‘regions’ mentioned in L188-L196 are selected. Relevant information should be disclosed in the methodology section. Also, why are 12 regions selected first, and then only 9 are used (L197)? Please, provide the necessary explanations.

Response:

Adopting the framework established by Jacobson et al. (2007), NOAA CT2022 partitions the global ocean into 30 basins to represent large-scale circulation and biogeochemical dynamics. This basin-based approach groups regions by their internal coherence in physical processes—such as currents, upwelling, and mixing—and biogeochemical behaviors, including nutrient cycling and carbon uptake. We examined the seasonal variability and mean state of global CO₂ fluxes, excluding regions where flux sign reverses across seasons—an effect that may introduce substantial uncertainty in model–data comparisons—with particular emphasis on the 12 regions exhibiting the strongest oceanic CO₂ fluxes (L188-L196).

Of the 30 regions, those exhibiting seasonal flux sign reversals were excluded, leaving 12 regions for further analysis (L197–L222). These 12 regions are divided into two categories: (1) 9 characteristic regions where the model-simulated CO₂ fluxes are generally consistent with NOAA CT2022 (L197), and (2) 3 regions that exhibit notable discrepancies compared with NOAA CT2022 (L215).

Jacobson, A. R., Gruber, N., Sarmiento, J. L., Gloor, M. and Fletcher, S. E. M.: A joint atmosphere-ocean inversion for surface fluxes of carbon dioxide: I. methods and global-scale fluxes, Global.

RC1.11. In connection to the previous comment, section 3.2 focuses on the Pacific sink and source regions. Why these regions? Not only the methodological information is needed, but at this point also the overall objective becomes confusing. Are these test cases? Is the focus of the work to evaluate the global impact of wave and bubble-mediated mechanisms on CO₂ flux? Or only focus on certain regions.

Response:

To demonstrate that the sea state–dependent K_w (Deike and Melville, 2018) provides a more suitable estimate of CO₂ flux than the wind-only K_w (Wanninkhof, 1992) under high-wind conditions, we selected two regions with contrasting wind regimes (one with over 30% of $U_{10} > 10 \text{ m s}^{-1}$ and another with all $U_{10} < 10 \text{ m s}^{-1}$). These regions also exhibit stable and significantly positive or negative oceanic CO₂ fluxes, allowing us to compare the correlation between K_w and U_{10} , as shown in Fig. 5 for (a) WP (160–180°E, 35–40°N; Fig. 5a) and (b) EP (230–250°E, 0–5°S; Fig. 5b).

The study also examines the difference between the monthly normal conditions means ($H_s < 1.5\text{m}$) and the K_w derived from averaging daily data with $H_s > 1.5\text{m}$, to assess whether the observed phenomenon reported by Gutiérrez-Loza et al. (2022) can also be reproduced in the model. While the relationship between K_w and U_{10} —when based on monthly normal conditions means ($H_s < 1.5\text{m}$) and daily data filtered for $H_s > 1.5\text{m}$ (enhanced conditions) and then aggregated into 30-year monthly averages—substantially diminishes differences in K_w at the same U_{10} . However, short-term (30-min) observations indicate that K_w can be up to twice as high under similar wind speeds (Gutiérrez-Loza et al., 2022, Fig. 7).

RC1.12. It is interesting to assess the impact of waves and bubbles in terms of the total flux (e.g. section 3.3). This has a lot of potential in terms of the relevance of including waves and wave-mediated processes in models to address carbon budgets, but also in terms of the process understanding. Posing questions like is the wave effect equally significant for source and sink regions? What does that represent for the global ocean carbon sink? Does integrating waves into models could bring global carbon sink estimates closer to observational-based estimates? All these questions are incredibly relevant and possible to address in this study.

Response:

We thank the reviewer for recognizing the relevance of this study. We will strive to address key questions regarding the impact of waves on ocean CO₂ flux. The following provides point-by-point responses to the reviewer's questions.

(1) the wave effect equally significant for source and sink regions?

Response:

The wave effect is most pronounced in tropical and subtropical regions, particularly in areas characterized by above-moderate wind speeds but high H_s, such as the tropical central Pacific in the Northern Hemisphere and the tropical Indian Ocean in the Southern Hemisphere, as highlighted by the white dashed borders in Fig. RC1.12.1(b). Additionally, within 30°N–30°S, K_w in the POP2-waves simulation increases by more than 40% relative to B-CTL. This region exhibits both positive and negative CO₂ fluxes but is predominantly a source (positive CO₂ flux).

Comparing Fig. 2(a)–(b) with Fig. RC1.12.1(b) and (d), the wave effect is more pronounced for positive CO₂ flux than for negative CO₂ flux. This is because regions with positive CO₂ flux have a larger air–sea dpCO₂, whereas regions with negative CO₂ flux have a smaller dpCO₂. As a result, the multiplicative effect enhances the impact of POP2-waves more strongly in regions with positive CO₂ flux.

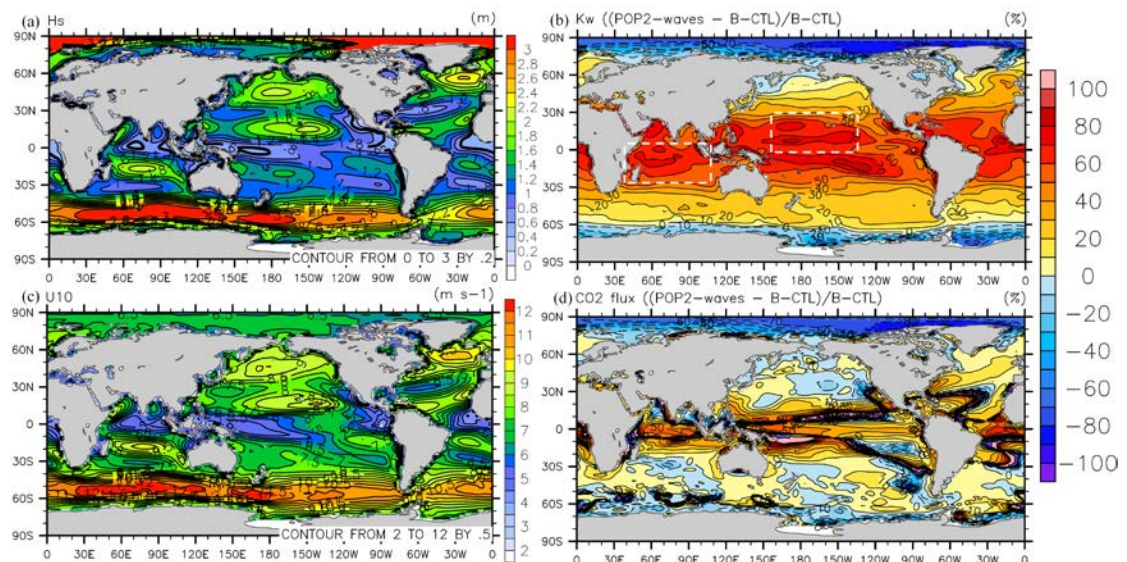


Figure RC1.12.1. Thirty-year mean fields of (a) significant wave height (H_s), (b) the difference in gas transfer velocity (K_w) between POP2-waves and B-CTL, (c) 10-m wind speed (U₁₀), and (d) the difference in CO₂ flux between POP2-waves and B-CTL. The white dashed borders in panel (b) highlight regions with larger K_w differences associated with higher H_s and U₁₀.

(2) What does that represent for the global ocean carbon sink?

Response:

As noted in the conclusion, under the dpCO₂-driven negative feedback associated with the interaction between CO₂ fluxes and the carbonate–pH system, POP2-waves show increases of 11.8%, 41.6%, and 1.8% in the negative CO₂ flux regions, positive CO₂ flux regions, and the global ocean carbon sink, respectively, compared to B-CTL.

(3) Does integrating waves into models could bring global carbon sink estimates closer to observational-based estimates?

Response:

Overall, incorporating waves into the model can bring global carbon sink estimates closer to NOAA CT2022. However, because it increases both positive and negative CO₂ flux regions globally, the net change in the global carbon sink is only 1.8%, due to the compensating effects between positive and negative contributions.

RC1.13. While the results focus on the ‘kinematic’ part of the flux, assessing the effect of waves and bubbles on the gas exchange, the discussion section largely focuses on the ‘thermodynamic’ component of the flux, and the links between physics and biogeochemistry. Large parts of the discussion are written as introductory concepts (e.g. L334- 338), of course, because previously the focus was on the kinematic properties (i.e. waves, bubbles, wind, u^ , K_w , etc.). Other parts are largely written as results, describing additional figures and introducing new findings, correlations, uncertainty analysis. Despite being interesting, all this is not a discussion. I encourage the authors to reconsider the key objectives and structure of the manuscript.*

Response:

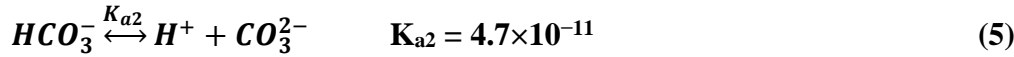
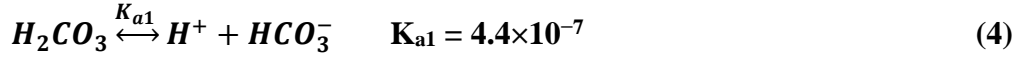
Thank you for your comment. Completing this interdisciplinary manuscript was challenging. It required programming expertise to port the wave module from other models into the CESM1 framework, as well as effective coupling between the wave, atmosphere, sea ice, and ocean components. The study also involved concepts from kinematics, thermodynamics, and biogeochemistry. All of the coding and most of the writing were carried out by the first author, I also aimed to clearly explain the underlying physical principles to make the manuscript as complete as possible.

The primary contribution of this study lies in its online coupling framework, which explicitly incorporates wave effects into air–sea CO₂ flux simulations,

thereby capturing the ocean's buffering capacity. In contrast, treating dpCO_2 and wave-induced K_w independently leads to a substantial overestimation of air–sea CO_2 fluxes when compared to online coupling POP2-waves simulations (section 4.3).

Lines 334–338 have been rewritten as follows:

The marine carbonic acid system is a nonlinear, coupled system governed by CO_2 dissolution equilibrium, ($\text{CO}_{2(aq)} + \text{H}_2\text{O} \xrightleftharpoons{K_H} \text{H}_2\text{CO}_{3(aq)}$), where the Henry's constant (K_H) for CO_2 in water at 25°C is approximately 3.4×10^{-2} (m/atm), two-step dissociation reactions, and the conservation of the total dissolved inorganic carbon (DIC) and total alkalinity (TA), ultimately determining pH and the distribution of carbonate species. The H_2CO_3 has two hydrogen ions and dissociates in two steps:



The DIC can be expressed as:

$$\begin{aligned} \text{DIC} &= [\text{H}_2\text{CO}_3] + [\text{HCO}_3^-] + [\text{CO}_3^{2-}] \\ &= K_H p\text{CO}_2^w + \frac{K_{a1} K_H p\text{CO}_2^w}{[\text{H}^+]} + \frac{K_{a1} K_{a2} K_H p\text{CO}_2^w}{[\text{H}^+]^2} \\ &= K_H p\text{CO}_2^w \left(1 + \frac{K_{a1}}{[\text{H}^+]} + \frac{K_{a1} K_{a2}}{[\text{H}^+]^2} \right) \\ &= K_H p\text{CO}_2^w ([\text{H}^+]^2 + K_{a1} [\text{H}^+] + K_{a1} K_{a2}) / [\text{H}^+]^2 \end{aligned} \quad (6)$$

The marine carbonate system describes the distribution of DIC among its chemical species in seawater and is jointly governed by TA and pH. From Eq. (6), if the oceanic $p\text{CO}_2^w$ and pH are known, the DIC can be determined, conversely, $p\text{CO}_2^w$ can be inferred from DIC. TA is defined as the sum of the proton-neutralizing capacities of all weak acid anions in seawater (Dickson, 1981) and can be expressed as:

$\text{TA} = [\text{HCO}_3^-] + 2[\text{CO}_3^{2-}] + [\text{B}(\text{OH})_4^-] + [\text{OH}^-] + [\text{HPO}_4^{2-}] + 2[\text{PO}_4^{3-}] + [\text{SiO}(\text{OH})_3] + [\text{NH}_3] + [\text{HS}^-] - [\text{H}^+] - [\text{H}_3\text{PO}_4]$. In the POP2-waves framework, TA, pH and biogeochemistry are also used to calculate $p\text{CO}_2$. The biogeochemical module of POP2 (MARBL) updates TA in each grid cell by solving a coupled transport–reaction equation (Long et al., 2021). The average pH of the ocean is currently around 8.1 (Fig. 8c), reflecting slightly alkaline conditions. Within the DIC system,

bicarbonate ions (HCO_3^-) are the dominant species because the prevailing pH lies between pK_{a1} and pK_{a2} . However, continued uptake of atmospheric CO_2 drives a decline in pH, a process termed ocean acidification.

We have clarified the key objectives and revised the manuscript structure accordingly. Please refer to the updated version for these changes.

Reference

- Dickson, A. G.: An exact definition of total alkalinity and a procedure for the estimation of alkalinity and total inorganic carbon from titration data, *Deep-Sea Res.*, 28A (6), 609-623, [https://doi.org/10.1016/0198-0149\(81\)90121-7](https://doi.org/10.1016/0198-0149(81)90121-7), 1981.
- Long, M. C., Moore, J. K., Lindsay, K., Levy, M., Doney, S. C., Luo, J., Krumhardt, K. M., Letscher, R. T., Grover, M., and Sylvester, T.: Simulations with the marine biogeochemistry library (MARBL). *J. Adv. Model. Earth Sy.*, 13(12), e2021MS002647. <https://doi.org/10.1029/2021MS002647>, 2021.

RC1.14. In the conclusions, the authors point to significant challenges in the POP2-waves coupling. However, these are not described or discussed in the paper. It is also mentioned that the results are used to compare CO2 fluxes (including wave and bubble-mediated effects) with NOAA CT2022, but this is only very briefly done. The conclusions must be consistent with the content of the rest of the manuscript.

Response:

Coupling a wave model into an ocean circulation model to simulate air–sea CO_2 flux presents substantial challenges arising from multi-scale physical processes, cross-component coupling, and nonlinear carbon cycle feedbacks. These challenges can be categorized into three main aspects: model coupling and implementation, underlying theoretical processes and data analysis (kinematics, thermodynamics, and biogeochemistry), and model validation and uncertainty.

Figure 11 consolidates key findings from previous sections to synthesize the regions of maximum negative and positive air–sea CO_2 flux (WP: 160–180°E, 35–40°N and EP: 230–250°E, 0–5°S, respectively), organized by winter and summer. As detailed in Section 3.1, the figure summarizes the mean and seasonal variations in air–sea CO_2 flux. Furthermore, it incorporates the changes in pCO_2^w and pH between the POP2–waves and B–CTL experiments (described in Section 4.1 and shown in Fig. 8), illustrating how the coupled model reduces high pCO_2^w by over 10 ppm in the EP and induces pH

differences of approximately ± 0.01 . Finally, Fig. 11 includes thermodynamic SST information, with colors highlighting the contrasts between the WP and EP regions, thereby illustrating the relationship between air–sea CO₂ flux and SST described in Section 4.2 and Fig. 9c.

Technical corrections:

RC1.15. Use ‘biogeochemistry’ not ‘geochemistry’

Response:

Thank you for your comment. Please see revised manuscript for the change.

RC1.16. Use ‘air-sea flux’ instead of ‘sea-air flux’

Response:

Thank you for your comment. Please see revised manuscript for the change.

RC1.17. L55: ‘slow conduction’ can be removed from the sentence has here the main topic is on mass transport which under non-turbulent conditions ‘occurs through molecular diffusion’.

Response:

We have removed ‘slow conduction’ from the sentence. Please see revised manuscript for the change.

RC1.18. L55: Avoid using ‘sources and sinks of CO₂ flux’. Either refer to a region as a ‘source or sink of CO₂’, or use ‘positive or negative CO₂ flux’, but there is no such thing as a source or sink of the flux.

Response:

We use “sources and sinks” to refer to an increase in magnitude in both positive and negative CO₂ flux regions. Here, “positive” and “negative” indicate only the direction of air–sea dpCO₂, i.e., from the ocean to the atmosphere or vice versa. For example, the CO₂ flux simulated by POP2-waves is stronger than that of B-CTL across both positive and negative CO₂ flux regions.

We have removed the phrase “sources and sinks of CO₂ flux” and replaced it with “positive or negative CO₂ flux,” except in the cases described above, where “and” is used to indicate enhancement in both regions.

*RC1.19. L179: 'mean air-sea CO2 flux' or 'mean atmosphere-ocean CO2 flux'
instead of 'mean ocean CO2 flux'.*

Response:

Thank you for your comment. Please see revised manuscript for the change.